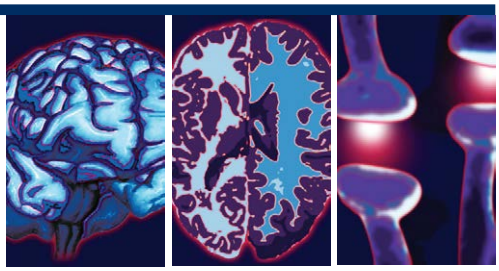

Contribution of Sodium-Calcium Exchanger Isoform-3 in $A\beta_{1-42}$ Induced Cell Death

Henok Kessete Afewerky[1,2,4,5,†], Hao Li[3,4], Pei Pang[3,4], Tongmei Zhang[3,4], Youming Lu[3,4,†]

ABSTRACT

$A\beta_{1-42}$ is a peptide which can alter intracellular calcium ($Ca2^{+}$) homeostasis and subsequently cause cell death. The molecular mechanisms underlying $A\beta_{1-42}$-induced Ca^{2+} dyshomeostasis and neurodegeneration are not fully elucidated. The third isoform of the sodium-calcium exchanger (NCX) family, NCX3, plays a vital role in adjusting excitable cells Ca^{2+} homeostasis. In this study, using NCX3 stably transfected baby hamster kidney (BHK) cells, we aim to study the role of NCX3 against $A\beta_{1-42}$ induced cell death. Our result demonstrates that NCX3 stably transfected cells (BHK-NCX3) are more resistant to $A\beta_{1-42}$ aggregation compared to their wild types (BHK-WT). The increased cellular loss in BHK-WT was correlated to increased cytoplasmic Ca^{2+} concentration ($[Ca^{2+}]_i$) induced by $A\beta_{1-42}$. These results present that NCX3 protects against $A\beta_{1-42}$-induced cell death and proclaim NCX3 and its downstream molecular pathways as critical components that take part in $A\beta_{1-42}$ neurotoxicity. Our study substantiates molecular events through which $A\beta_{1-42}$ can induce neurodegeneration such as Alzheimer's disease and marks potential targets to slow down neuropathogenesis.

Key words

Amyloid-beta, Sodium–calcium exchanger, Baby Hamster Kidney Cells, Alzheimer's disease

Introduction

Amyloid-beta (Aβ) peptides are metabolic products consisting of 38 to 43 amino acids, which exists in two prevalent isoforms: soluble $A\beta_{1-40}$ (~80-90%) and insoluble $A\beta_{1-42}$ (~5-10%) [1,2]. Monomers of $A\beta_{1-40}$ are much more ubiquitous than the aggregation-prone and toxic $A\beta_{1-42}$ species. Aβ peptides originate from sequential cleavage of the Aβ precursor protein (APP) by the enzymatic actions of β-secretase and γ-secretase [3,4]. Its primacy has been evidenced in the 'amyloid cascade hypothesis', which postulates that the accumulation of Aβ (resulting from excessive production, distorted processing or unbalance between production and clearance) is the potential mechanism that leads neurodegeneration in Alzheimer's disease (AD) [5]. However, the mechanism of pathogenicity for Aβ has not been fully elucidated. In the last decade, several studies have reported that Aβ is implicated in several pathological

[1]Department of Neurobiology, School of Basic Medicine, Tongji Medical College, Huazhong University of Science and Technology, Wuhan 430030, China

[2]Department of Pathology and Pathophysiololgy, School of Basic Medicine, Tongji Medical College, Huazhong University of Science and Technology, Wuhan 430030, China

[3]Department of Physiology, School of Basic Medicine, Tongji Medical College, Huazhong University of Science and Technology, Wuhan 430030, China

[4]Institute for Brain Research, Collaborative Innovation Center for Brain Science, Huazhong University of Science and Technology, Wuhan 430030, China

[5]School of Allied Health Professions, Asmara College of Health Sciences, Asmara, Eritrea

[†]Author for correspondences: Henok Kessete Afewerky, Department of Neurobiology, School of Basic Medicine, Tongji Medical College, Huazhong University of Science and Technology, Wuhan, 430030, China, Tel: 0086-13260654649

[†]Author for correspondences: Youming Lu, Department of Physiology, School of Basic Medicine, Tongji Medical College, Huazhong University of Science and Technology, Wuhan, 430030, China, Tel: 0086-18171337550

conditions of the central nervous system, such as frontotemporal dementia (FTLD) [6,7] and AD [5,8,9]. These findings consistently pioneered the contribution of Ca^{2+} dishomeostasis in Aβ induced cell death [5,9].

The sodium–calcium exchanger (NCX) is a plasma membrane protein that plays a major role in the maintenance of Ca^{2+} and Na^{+} homeostasis in most excitable and non-excitable cells. NCX plays a significant role in neurons, where an alteration in cytosolic Ca^{2+} concentration represents a vital event in several physiological (e.g. synaptic transmission) and pathological phenomenon (e.g. AD) [5,10]. NCX can function in two modes of action which are referred to as the "Ca^{2+} outflow mode" and "Ca^{2+} inflow mode" [5,11]. The functioning mode, effectively the direction of exchange, depends on the Ca^{2+} and Na^{+} electrochemical gradients across the plasma membrane and on the membrane potential. The Ca^{2+} outflow mode of exchange (forward mode) is defined functionally as an outside Na^{+}-dependent Ca^{2+} outflow and an inside Ca^{2+}-dependent Na^{+}-inflow. The Ca^{2+} inflow mode of exchange (reverse mode) is usually defined as an inside Na^{+}-dependent Ca^{2+}-inflow and outside Ca^{2+}-dependent Na^{+}-outflow. Because of the lack of specific inhibitors, whether NCX contributes to both net Ca^{2+} inflow and net Ca^{2+} outflow under normal physiological conditions is not thoroughly elucidated. However, there is a common understanding that the exchanger plays a significant role in removing Ca^{2+} in various cell types [12-14]. Three isoforms of the exchanger (NCX1, NCX2, and NCX3) encoded by different genes have been cloned [5,15]. NCX1 is predominantly expressed in the heart and is common in excitable cells [16,17]. The NCX2 expression is limited to the brain and spinal cord [16,18], while NCX3 expression is confined to the central nervous system and skeletal muscle [16,19]. In situ hybridization studies using rodent brain depicted that NCX1, NCX2, and NCX3 mRNA are found dispersed in all brain regions including the hippocampus, a region mostly provoked in AD [5,20,21]. The operational roles of each isoform in neurons yet have to be examined. Recently, Henok et al. [5] presented the protective role of NCX against ischemic damage and its role for cognitive function. Moreover, this study specifically implied that NCX3 is a potential molecular target in AD therapy.

In the current study, using NCX3 stably transfected baby hamster kidney (BHK) cells, we aimed to study whether NCX3 contributes against cell death induced by the $Aβ_{1-42}$. We determined that BHK-NCX3 are more resistant to $Aβ_{1-42}$ aggregation compared to wild-type (BHK-WT) cells which do not constitutively express NCX3 [22,23], as revealed by the staining with calcein-AM (a marker of living cells) and propidium iodide (a marker of non-viable cells) **(Figure 1A)**. This increase in $Aβ_{1-42}$-induced death in BHK-WT cells correlate with a significant increase in intracellular Ca^{2+} concentration ($[Ca^{2+}]_i$) which subsequently contributes toward mitochondrial dysfunction and then ATP depletion [24,25]. In conclusion, our determinations contemplate that NCX3 might offer a therapeutic target to decelerate neurodegenerations such as AD.

Materials and Methods

■ Materials

Baby Hamster Kidney (BHK) Cells were obtained from BioVector NTCC Inc. (GNHa10; Beijing, China). $Aβ_{1-42}$ (ab120301), Rabbit polyclonal anti-NCX3 antibody (1:2000) (ab84708) and mouse monoclonal anti-tubulin (1:1000) (ab7751) were purchased from Abcam (Wuhan, Hubei, China). Nutrient Mixture F-12 (Hams' F-12) (11320082), Dulbecco's Modified Eagle's Medium (DMEM) (12491-015), Trypsin-EDTA 0.25% (25200056), Penicillin-streptomycin (15140122), Heat-inactivated fetal bovine serum (FBS) (16000044), fluorescent dyes (i.e. Trypan Blue (15250061), and DNA binding dye (Hoechst-33258)), Poly-L-lysine (132706), and Protease inhibitor cocktail II (78437) as well as all other unmentioned materials, were all from Thermo Fisher Scientific (Wuhan, Hubei, China).

■ Cell culture

The baby hamster kidney (BHK) cells were grown on plastic dishes in a mix of DMEM and Ham's F12 media (1:1) supplemented with 5% fetal bovine serum, 100 U/ml penicillin, and 100 µg/ml streptomycin. Cells were cultured in a humidified 5% CO_2 atmosphere; the culture medium was changed every 2 days. For microfluorimetric studies, cells were plated on glass coverslips (102260, Thermo Fisher Scientific) coated with poly-L-lysine (30 µg/ml) and used at least 12 hours after plating [26].

■ Cell transfection

In the next day following the seeding of the cells to 70-90% confluence in a flask, complete

medium (DMEM solution) was replaced with Opti-MEM™ medium. Cells were transfected by adding complex mix of NCX3 plasmid (5 µl) diluted in a solution of Lipofectamine™ as described in the manufacturer's protocol.

■ $A\beta_{1-42}$ peptide treatment

$A\beta_{1-42}$ was prepared as 0.1 mg/0.1 ml stock solution in sterile phosphate buffer solution (PBS) incubated at 37°C for 24 hours to enhance aggregation, and stored at -20°C. Stock solution was then directly diluted in cell culture media to give the desired experimental concentrations (1 µM/10 µM).

■ Cell viability count

Following 24 h treatment with 1 µM $A\beta_{1-42}$ and following 6 h treatment with 10 µM $A\beta_{1-42}$, at various time points, cells were incubated in an aliquot containing 0.4% Trypan Blue at room temperature (23°C) for 15 min and then blue cells were counted on a haemocytometer. The percentage of Trypan Blue positive cells was averaged over five fields' total number of cells.

■ Assessment of nuclear morphology

Nuclear morphology was evaluated by using the fluorescent DNA-binding dye Hoechst-33258. To this aim, cells were fixed in 4% paraformaldehyde and incubated for 5 minutes in PBS containing 1 µg/ml Hoechst-33258 at 37°C. Coverslips were mounted on glass slides and observed with the Olympus fluorescence microscope 1X71S1F-3 (Tokyo, Japan). Digital images were taken with a DP72 camera (Olympus, Tokyo, Japan), stored on the hard-disk of a Pentium III computer, and analyzed with the Image-Pro Plus 4.5 software (Media Cybernetics Inc, Silver Spring, MD, USA). Pathological nuclei were characterized

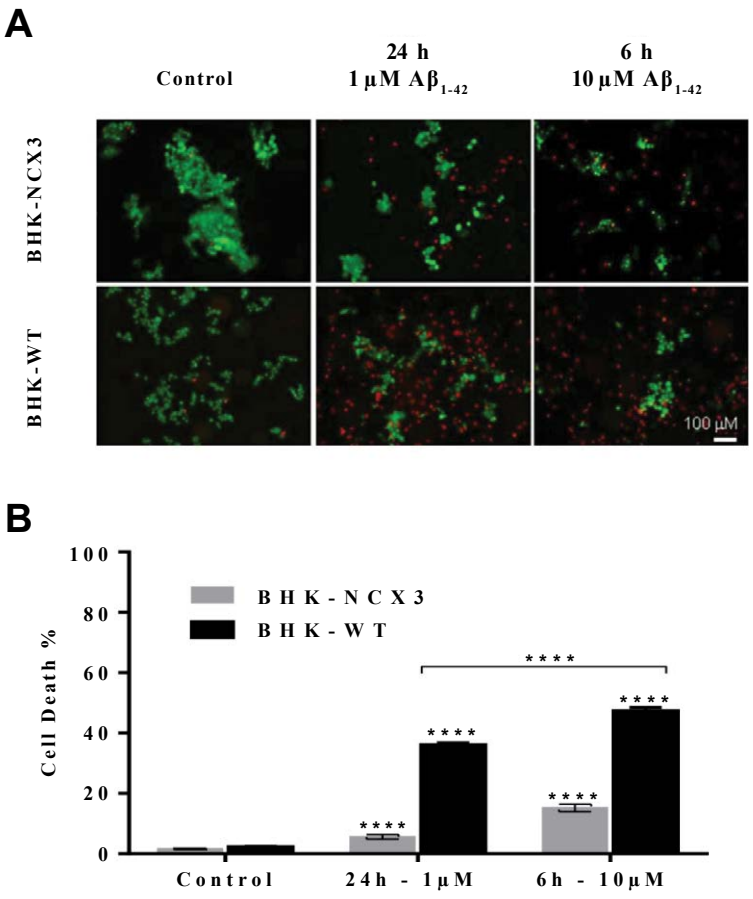

Figure 1: Effect of $A\beta_{1-42}$ treatment on cell viability in BHK-WT and BHK-NCX3 cells

A: Representative fluorescent images of BHK-WT and BHK-NCX3 cells double stained with calcein-AM (a marker of living cells) and propidium iodide (a marker of non-viable cells) in control conditions (DMSO-24 h), following 24 h treatment with 1 µM $A\beta_{1-42}$, and following 6 h treatment with 10 µM $A\beta_{1-42}$.

B: Bar graph illustrating cell death in BHK-WT and BHK-NCX3 cells following $A\beta_{1-42}$ exposure (1 µM for 24 h and 10 µM for 6 h), and in vehicle control condition treated with solvent DMSO for 24 h. **** $P < 0.0001$ vs. control condition; **** $P < 0.0001$ vs. BHK-WT cells. Each bar represents the mean (± SEM) of dozen different experimental values studied in four independent experimental sessions.

by chromatin condensation (pyknosis) and fragmentation, or by decreases and increases in size [27,28].

■ Immunoblotting

After treatment, cells were lysed with a buffer containing 20 mM Tris–HCl (pH 7.5), 10 mM NaF, 1 mM phenylmethylsulfonyl fluoride, 1% NONIDET P-40, 1 mM Na_3VO_4, 0.1% aprotinin, 0.7 mg/ml pepstatin and 1 µg/ml leupeptin. Samples were cleared by centrifugation and supernatants were used for Western blot. Protein concentration in supernatants was determined by Bradford method [29]. Protein samples (50 µg) were analyzed on 8% sodium dodecyl sulfate polyacrilamide gel with 5% sodium dodecyl sulfate stacking gel (SDS-PAGE) and electrotransferred onto Hybond ECL nitrocellulose paper (LC2006, Thermo Fisher Scientific). Membranes were blocked with 5% nonfat dry milk in 0.1% Tween 20 (TBS-T; 2 mmol/l Tris–HCl, 50 mmol/l NaCl, pH 7.5) for 1 h at room temperature and subsequently incubated overnight at 4°C in the blocked buffer with rabbit polyclonal NCX3 antibody (1:2000) [17,30].

The membranes were washed with 0.1% Tween 20 and incubated with horseradish peroxidase (HRP)-conjugated anti-rabbit IgG (1:1000) (ab21058, Abcam) for 1 h. Immunoreactive bands were detected with the ECL. The optical density of the bands (normalized with those of actin) was determined by Chemi Doc Imaging System (Biorad).

■ Statistical analysis

Statistical analysis was performed on actual cell counts using Prism software (GraphPad 6 software, San Diego, CA). All experiments were performed at least three times on separate days. On individual days, experiments were performed in triplicate and averaged to form a single experiment unit. Analyses were performed using one-way analysis of variance (ANOVA) followed by Student t test, and differences were considered to be statistically significant when P values were <.05. Data are presented as means ± standard error of the mean (SEM).

Results

To investigate the contribution of NCX3 against $A\beta_{1\text{-}42}$-induced cell death, NCX3 cDNA was stably transfected in BHK cells, which do not constitutively express NCX isoforms [16]. In both cell lines, BHK-WT and BHK-NCX3, toxicological damages caused by a 24 h exposure of 1 µM $A\beta_{1\text{-}42}$ was compared to an acute exposure of 6 h with a 10 times higher dose of $A\beta_{1\text{-}42}$ [31]. The results of this study, demonstrated that the NCX3 gene product may play a relevant role in the cells resistance to $A\beta_{1\text{-}42}$-induced death. Whereby, BHK-WT cells were more susceptible to $A\beta_{1\text{-}42}$ cytotoxicity than BHK-NCX3 exposed to 1 µM $A\beta_{1\text{-}42}$ for 24 h (36.1 ± 0.7% of cell death in BHK-WT vs. 5.6 ± 0.8% of cell death in BHK-NCX3; P<0.0001) or 10 µM $A\beta_{1\text{-}42}$ for 6 h (47.4 ± 1.1% of cell death in BHK-WT vs. 15.2 ± 1.3% of cell death in BHK-NCX3; P<0.0001) **(Figure 1B)**. In controlled conditions, cell viability was similar in both the transfected and wild type BHK cells as revealed by the haemocytometer cell count.

To evaluate BHK-WT and BHK-NCX3 cells resistance to $A\beta_{1\text{-}42}$-induced death at 72 h, these cells were exposed to 10 µM $A\beta_{1\text{-}42}$ following the seeding of the cells to 70-90% confluence. At this period of time, BHK-NCX3 cells were more resistant to the insult as compared to BHK-WT cells as revealed by the staining with calcein-AM and propidium iodide microscopic fluorescence **(Figure 2A)**; and Trypan Blue cell viability count **(Figure 2B)**. In addition, BHK-WT cells showed hastened $A\beta_{1\text{-}42}$-induced abnormal nuclear morphology at 48 h, as detected by Hoechst 33258 (data not shown). Here we present substantiative evidence that BHK cells stably expressing NCX3 isoform are more resistant to $A\beta_{1\text{-}42}$-induced cell death.

Most importantly, immunoblot analysis revealed that following 10 µM $A\beta_{1\text{-}42}$ peptide treatment, the NCX3 native band, detected at ~105 kDa, decreased at 12, 24, 48, and 72 h, whereas the proteolytic band, migrating at ~75 kDa, increased progressively from 12 to 48 h **(Figure 3)**. Moreover, coincident with the rapid rise in cell death, interestingly the $A\beta_{1\text{-}42}$-induced proteolytic band abruptly dropped after 48 h of the peptide treatment. These results demonstrate the effects of $A\beta_{1\text{-}42}$ on NCX3.

Discussion

Conceptually, physiological Aβ concentrations are necessary for normal synaptic plasticity and memory to occur [32,33]. But, previous lines of research using primary neurons have shown that abnormal Aβ concentration can induce behavioral changes and loss of neurons through the apoptosis program [34,35]. However, the

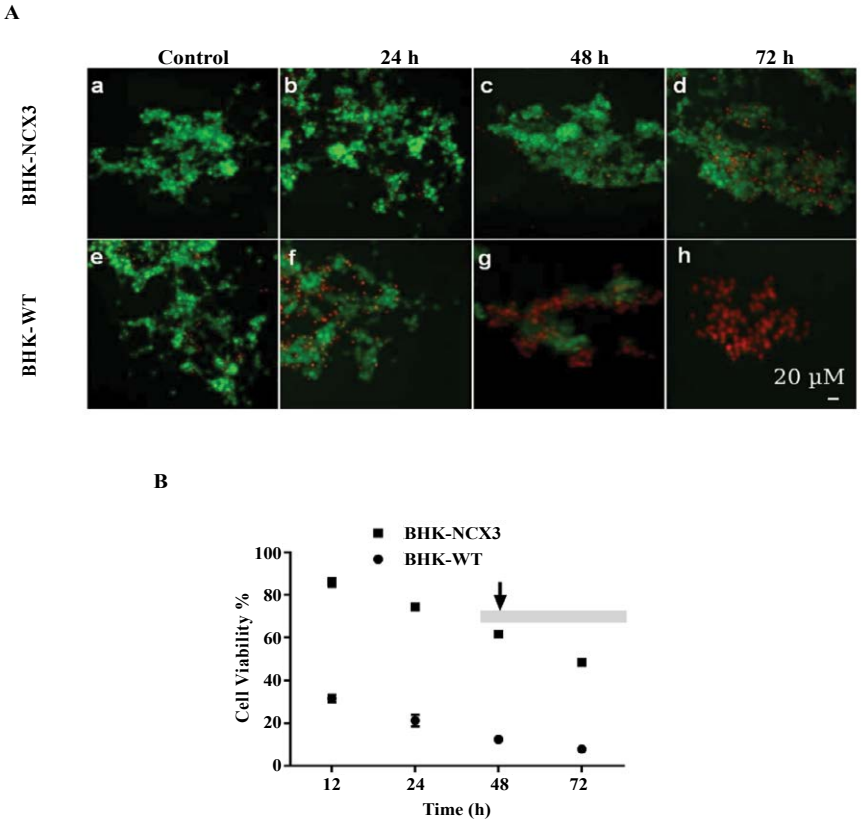

Figure 2: Viability of BHK-WT and BHK-NCX3 cells following treatment with 10 µM $A\beta_{1-42}$ at intervals for 3 days.

A: Representative fluorescent images double stained with calcein-AM (a marker of living cells) and propidium iodide (a marker of non-viable cells) acquired under control conditions and after 24, 48 and 72 h of $A\beta_{1-42}$ exposure in the BHK-NCX3 (***a***–***d***) and in the BHK-WT (***e***–***h***) cells.

B: Graph illustrating cell death in BHK-WT and BHK-NCX3 cells after 12, 24, 48, and 72 h of 10 µM $A\beta_{1-42}$ exposures. Each bar represents the mean (± SEM) of dozen different experimental values studied in four independent experimental sessions. The arrow marks time after which the $A\beta_{1-42}$-induced proteolytic band dropped sharply.

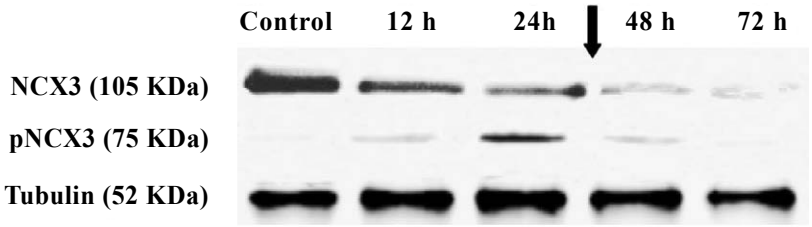

Figure 3: Effect of $A\beta_{1-42}$ on NCX3 inactivation and on the consequent formation of NCX3 proteolytic fragment in BHK-NCX3 cells (Representative Immunoblot of NCX3 inactivation and its proteolytic fragment (pNCX3) formation; in BHK-NCX3 cells under control conditions, and after 12, 24, 48, and 72 h of 10 µM $A\beta_{1-42}$ exposures)

molecular mechanism(s) by which extracellular Aβ peptide damages neurons is still mostly unknown.

One of the main mechanisms responsible for the neurotoxicity by Aβ may be that Aβ interacts with cell membrane components which further directly damages and/or enhances the vulnerability of neurons [36]. To address this, NCX3 stably transfected BHK cells which otherwise do not constitutively express NCX isoforms were cultured.

Using BHK cells expressing brain specific NCX3 isoform, we demonstrate that NCX3 plays an important role in $A\beta_{1-42}$-induced cell death. Our findings reveal that NCX3 stably transfected BHK cells show significant resistance to $A\beta_{1-42}$-

induced plaque formation and death compared to BHK-WT. These results are consistent to previous reports were NCX3$^{+/+}$ primary brainstem cultures exposed to $A\beta_{1-42}$ showed resistance compared to neurons obtained from wild-type mice [37,38]. Furthermore, in most studies, Ca^{2+} dysregulation following to $A\beta_{1-42}$ aggregation was the leading cause of neuronal cell death [39,40]. In the current study, results present two important findings. First, NCX3 expression unprovoked $A\beta_{1-42}$ induced toxicity in BHK cells; whereby NCX3 genetic transfection in to BHK cells was found protective against $A\beta_{1-42}$-induced cell death. BHK-NCX3 cells treated with $A\beta_{1-42}$ showed significant resistance to cell death compared to BHK-WT.

Second, we showed that following $A\beta_{1-42}$ treatment, inhibition of NCX3 expression and ultimately cell death **(Figures 2 and 3)** over a period of time. We can speculate that the increase of cell death observed in BHK-NCX3 cells in after 48 h of treatment with $A\beta_{1-42}$ peptide was caused by the peptide fair specificity for the NCX3 functional modes of action (Ca^{2+} exchange) and its ability to inhibit the normal Krebs cycle complex I in the mitochondrial respiratory chain [30,41]. This speculation is supported by our observation in BHK-NCX3 cells, where NCX3 expression is totally abolished following to 48-72 h $A\beta_{1-42}$ treatment.

It may be premature to call at this point, but in all probability, mitochondrial dysfunction and accordingly limited ATP production were the contributing factors to the compromised BHK-NCX3 cells survival following $A\beta_{1-42}$ exposure. The extent to which the mitochondrial dysfunction and the decreased ATP production are a consequence of NCX3 inhibition by $A\beta_{1-42}$ is not yet fully elucidated. However, previous studies showed that, mitochondria play a major role in sequestration of Ca^{2+} [42,43] and since Ca^{2+} is a positive effector of mitochondrial function [44], any perturbation in mitochondrial and/or cytosolic Ca^{2+} homeostasis have major consequences to cell function. It is plausible that $A\beta_{1-42}$ induces a positive-feedback loop between mitochondrial dysfunction and cytoplasmic Ca^{2+} dysregulation. Overall, these findings present NCX3 protein as a substantial molecular target that may have a potential therapeutic value in modulating $A\beta_{1-42}$ induced pathogenesis. Further studies are needed to elucidate the exact sequence of events between mitochondrial and Ca^{2+} pathways of $A\beta_{1-42}$ cytotoxicity.

Conclusion

Indeed, BHK-NCX3 cells, unlike BHK-WT cells are able to better survive $A\beta_{1-42}$ aggregation possibly by virtue of the NCX3 Ca^{2+}-buffering properties in conditions of ATP depletion [5,15]. Therefore, our findings assert the protective role of NCX3 against $A\beta_{1-42}$-induced cell death, and suggest reduced NCX3 and its downstream molecular pathways as key factors involved in $A\beta_{1-42}$-induced neuropathogenesis such as Alzheimer's disease. Further studies, including in-vivo animal experiments, are necessary for the determination of the actual contribution of NCX3 in $A\beta_{1-42}$-induced human neuronal death.

Conflicts of Interest

The authors declare no conflict of interest.

Acknowledgments

This work was supported by the Chinese Government Scholarship–Chinese University Program (No.2018GXZ024192) and National Natural Science Foundation of China (No.31500832).

Author's Contributions

Henok Kessete Afewerky conceived and designed the study, performed the experiments, analyzed the data and wrote the manuscript. Tongmei Zhang helped to design the experiments. Hao Li and Pei Pang helped to analyze the data. Youming Lu supervised the study.

Abbreviations

Aβ: Amyloid-beta; NCX: Sodium-calcium exchanger; BHK: Baby Hamster Kidney cells; AD: Alzheimer's disease

References

1. Gandy S. APP processing, A beta-amyloidogenesis, and the pathogenesis of Alzheimer's disease. *Neurobiol. Aging* 15(2), 253-256 (1994).
2. Zhang YW, Xu H. Molecular and cellular mechanisms for Alzheimer's disease: understanding APP metabolism. *Curr. Mol. Med* 7(7), 687-696 (2007).
3. Serrano-Pozo A, Frosch MP, Masliah E, *et al*. Neuropathological alterations in Alzheimer disease. *Cold. Spring. Harb. Perspect. Med* 1(1), a006189 (2011).
4. Xu X. Gamma-secretase catalyzes sequential cleavages of the AbetaPP transmembrane domain. *J. Alzheimers. Dis* 16(2), 211-224 (2009).
5. Henok KA, Zhang T, Hao Li, *et al*. Roles of sodium-calcium exchanger isoform-3 toward calcium ion regulation in Alzheimers disease. *J. Alzheimers. Dis. Parkinsonism* 6(7), 1-4 (2016).
6. Alcolea D, Vilaplana E, Suárez-Calvet M, *et al*. CSF sAPPbeta, YKL-40, and neurofilament light in frontotemporal lobar degeneration. *Neurology* 89(2), 178-188 (2017).
7. Kim BJ, Irwin DJ, Song D, *et al*. Optical coherence tomography identifies outer retina thinning in frontotemporal degeneration. *Neurology* 89(15), 1604-1611(2017).
8. Czeczor JK, McGee SL. Emerging roles for the amyloid precursor protein and derived peptides in the regulation of cellular and systemic metabolism. *J. Neuroendocrinol* 29(5) (2017).
9. Garcia-Ribas G, García-Ribas G, Carrió I, *et al*. PET biomarkers: Use of imaging techniques in Alzheimer disease and neurodegeneration clinical diagnosis. *Neurologia* 32(5), 275-277 (2017).
10. Bano D, Young KW, Guerin CJ, *et al*. Cleavage of the plasma membrane Na^+/Ca^{2+} exchanger in excitotoxicity. *Cell* 120(2), 275-285 (2005).
11. Hilge M. Ca^{2+} regulation of ion transport in the Na^+/Ca^{2+} exchanger. *J. Biol. Chem* 287(38), 31641-31649 (2012).
12. Michel LY, Hoenderop JG, Bindels RJ. Towards understanding the role of the Na(2)(+)-Ca(2)(+) exchanger isoform 3. *Rev. Physiol. Biochem. Pharmacol* 168(1), 31-57 (2015).
13. Pelzl L, Hosseinzadeh Z, Alzoubi K, *et al*. Impact of Na^+/Ca^{2+} exchangers on therapy resistance of ovary carcinoma cells. *Cell. Physiol. Biochem* 37(5), 1857-1868 (2015).
14. Sirabella R, Secondo A, Pannaccione A, *et al*. ERK1/2, p38, and JNK regulate the expression and the activity of the three isoforms of the Na^+ /Ca^{2+} exchanger, NCX1, NCX2, and NCX3, in neuronal PC12 cells. *J. Neurochem* 122(5), 911-922 (2012).
15. Linck B, Zhiyong Q, Zhaoping H, *et al*. Functional comparison of the three isoforms of the Na^+/Ca^{2+} exchanger (NCX1, NCX2, NCX3). *Am. J. Physiol* 274(2), 415-423 (1998).
16. Minelli A, Castaldo P, Gobbi P, *et al*. Cellular and subcellular localization of Na^+-Ca^{2+} exchanger protein isoforms, NCX1, NCX2, and NCX3 in cerebral cortex and hippocampus of adult rat. *Cell. Calcium* 41(3), 221-234 (2007).
17. Thurneysen T, Nicoll DA, Philipson KD, *et al*. Sodium/calcium exchanger subtypes NCX1, NCX2 and NCX3 show cell-specific expression in rat hippocampus cultures. *Brain. Res. Mol. Brain. Res* 107(2), 145-156 (2002).
18. Jeon D, Yang YM, Jeong MJ, *et al*. Enhanced learning and memory in mice lacking Na^+/Ca^{2+} exchanger 2. *Neuron* 38(6), 965-76(2003).
19. Sokolow S, Manto M, Gailly P, *et al*. Impaired neuromuscular transmission and skeletal muscle fiber necrosis in mice lacking Na/Ca exchanger 3. *J. Clin. Invest* 113(2), 265-273 (2004).
20. Annunziato L, Pignataro G, Boscia F, *et al*. ncx1, ncx2, and ncx3 gene product expression and function in neuronal anoxia and brain ischemia. *Ann. N. Y. Acad. Sci* 1099(1), 413-426 (2007).
21. Canitano A, Papa M, Boscia F, *et al*. Brain distribution of the Na^+/Ca^{2+} exchanger-encoding genes NCX1, NCX2, and NCX3 and their related proteins in the central nervous system. *Ann. N. Y. Acad. Sci* 976(1), 394-404 (2002).
22. Jin J, Lao AJ, Katsura M, *et al*. Involvement of the sodium-calcium exchanger 3 (NCX3) in ziram-induced calcium dysregulation and toxicity. *Neurotoxicology* 45(1), 56-66 (2014).
23. Secondo A, Staiano IR, Scorziello A, *et al*., The Na^+/Ca^{2+} exchanger isoform 3 (NCX3) but not isoform 2 (NCX2) and 1 (NCX1) singly transfected in BHK cells plays a protective role in a model of in vitro hypoxia. *Ann. N. Y. Acad. Sci* 1099(1), 481-485 (2007).
24. Dodson M, Darley-Usmar V, Zhang J. Cellular metabolic and autophagic pathways: traffic control by redox signaling. *Free. Radic. Biol. Med* 63(1), 207-221 (2013).
25. Wang M, Li Y, Ni C, *et al*. Honokiol attenuates oligomeric amyloid beta1-42-induced Alzheimer's disease in mice through attenuating mitochondrial apoptosis and inhibiting the nuclear factor kappa-b signaling pathway. *Cell. Physiol. Biochem* 43(1), 69-81 (2017).
26. Secondo A, Staiano RI, Scorziello A, *et al*. BHK cells transfected with NCX3 are more resistant to hypoxia followed by reoxygenation than those transfected with NCX1 and NCX2: Possible relationship with mitochondrial membrane potential. *Cell. Calcium* 42(6), 521-535 (2007).
27. Ghavami S, Shojaei S, Yeganeh B, *et al*. Autophagy and apoptosis dysfunction in neurodegenerative disorders. *Prog. Neurobiol* 112(1), 24-49 (2014).
28. Salminen A, Kaarniranta K, Kauppinen A, *et al*. Impaired autophagy and APP processing in Alzheimer's disease: The potential role of Beclin 1 interactome. *Prog. Neurobiol* 106-107(1), 33-54 (2013).
29. Bradford MM. A rapid and sensitive method for the quantitation of microgram quantities of protein utilizing the principle of protein-dye binding. *Anal. Biochem* 72(1), 248-254 (1976).
30. Brustovetsky T, Brittain MK, Sheets PL, *et al*. KB-R7943, an inhibitor of the reverse Na^+ / Ca^{2+} exchanger, blocks N-methyl-D-aspartate receptor and inhibits mitochondrial complex I. *Br. J. Pharmacol* 162(1), 255-270 (2011).
31. Lanz TA, Wood KM, Richter KE, *et al*. Pharmacodynamics and pharmacokinetics of the gamma-secretase inhibitor PF-3084014. *J. Pharmacol. Exp. Ther* 334(1), 269-277 (2010).
32. Puzzo D, Arancio O. Amyloid-beta peptide: Dr. Jekyll or Mr. Hyde?. *J. Alzheimers. Dis* 33(1), 111-120 (2013).
33. Wen J, Fang F, Guo SH, *et al*. Amyloid beta-Derived Diffusible Ligands (ADDLs) Induce Abnormal Autophagy Associated with Abeta Aggregation Degree. *J. Mol. Neurosci* 64(2), 162-174 (2017).
34. Du YF, Yan P, Guo SG, *et al*. Effects of fibrillar Abeta(1-40) on the viability of primary cultures of cholinergic neurons and the expression of insulin signaling-related proteins. *Anat. Rec. (Hoboken)* 294(2), 287-294 (2011).
35. Zheng WH, Bastianetto S, Mennicken F, *et al*. Amyloid beta peptide induces tau phosphorylation and loss of cholinergic neurons in rat primary septal cultures. *Neurosci* 115(1), 201-211 (2002).
36. Perini G, Della-Bianca V, Politi V, *et al*. Role of p75 neurotrophin receptor in the neurotoxicity by beta-amyloid peptides and synergistic effect of inflammatory cytokines. *J. Exp. Med* 195(7), 907-918 (2002).
37. Wu A, Colvin RA. Characterization of exchange inhibitory peptide effects on Na^+/Ca^{2+} exchange in rat and human brain plasma membrane vesicles. *J. Neurochem* 63(6), 2136-2143 (1994).
38. Wu A, Derrico CA, Hatem L, *et al*. Alzheimer's amyloid-beta peptide inhibits sodi-

um/calcium exchange measured in rat and human brain plasma membrane vesicles. *Neurosci* 80(3), 675-684 (1997).

39. Lee WS, Tsai WJ, Yeh PH, *et al*. Divergent role of calcium on Abeta- and MPTP-induced cell death in SK-N-SH neuroblastoma. *Life. Sci* 78(11), 1268-1275 (2006) .

40. Piacentini R, Ripoli C, Leone L, *et al*. Role of methionine 35 in the intracellular Ca^{2+} homeostasis dysregulation and Ca^{2+}-dependent apoptosis induced by amyloid beta-peptide in human neuroblastoma IMR32 cells. *J. Neurochem* 107(4),1070-1082 (2008).

41. Roberts DE, Matsuda T, Bose R. Molecular and functional characterization of the human platelet $Na(^{+})$ /$Ca(^{2+})$ exchangers. *Br. J. Pharmacol* 165(4), 922-936(2012).

42. Einat H, Yuan P, Manji HK. Increased anxiety-like behaviors and mitochondrial dysfunction in mice with targeted mutation of the Bcl-2 gene: further support for the involvement of mitochondrial function in anxiety disorders. *Behav. Brain.* Res 165(2), 172-180 (2005).

43. Holmes A, Lit Q, Murphy DL, *et al*. Abnormal anxiety-related behavior in serotonin transporter null mutant mice: the influence of genetic background. *Genes. Brain. Behav* 2(6), 365-380 (2003).

44. Feissner RF, Skalska J, Gaum WE, *et al*. Crosstalk signaling between mitochondrial Ca^{2+} and ROS. *Front. Biosci. (Landmark Ed)* 14(1), 1197-1218 (2009).